EJAM
www.ejamjournal.com

Electronic Journal of Applied Mathematics

Research article

Mersin University Publishing
DOI: 10.61383/ejam.202533112
2025, Vol. 3, No. 3, 83–106

Efficient coupling technique for approximate and exact solutions of nonlinear Caputo fractional differential equations

Muhammad Imran Liaqat[1]

1. Abdus Salam School of Mathematical Sciences, Government College University, 68-B, New Muslim Town, Lahore 54600, Pakistan

*Corresponding author

Abstract

Complex phenomena such as anomalous diffusion, fractal structures, viscoelasticity, and chaotic dynamics are effectively described using fractional-order nonlinear models. Solving these nonlinear fractional models provides deeper insight into the mechanisms and behaviors underlying such processes. In this work, we develop a hybrid analytical technique for solving nonlinear fractional partial differential equations by coupling the residual function with the Laplace transform, referred to as the Laplace residual power series method (LRPSM). This method is constructed upon a modified fractional-order power series formulated within the framework of the Caputo derivative. The accuracy of the proposed approach is confirmed through absolute, relative, and residual error analyses. LRPSM efficiently determines the coefficients of series solutions using a simple limit principle at infinity, in contrast to well-established methods such as the variational iteration method, Adomian decomposition method, and homotopy perturbation method, which typically require complex integrations. Likewise, the classical residual power series method (RPSM) depends on higher-order derivatives, which become increasingly challenging in fractional settings. Since LRPSM avoids the use of Adomian's or He's polynomials for handling nonlinearities, it proves to be a more straightforward and computationally efficient alternative for obtaining accurate series solutions to nonlinear fractional problems.

Keywords: Fractional nonlinear model, Caputo derivative, Laplace transform, residual function, approximate solution, closed-form solution
MSC (2020): 22E70, 34A08, 35R11
Article history: Received 08 Jun 2025; Accepted 13 Sep 2025; Online 25 Sep 2025

1 Introduction to this Template

Fractional calculus, whose origins can be traced back to a discussion between Leibniz and L'Hôpital in 1695, has developed from a theoretical curiosity into a powerful mathematical framework for describing complex real-world systems. Its fundamental strength lies in the

Contact: Muhammad Imran Liaqat ✉ imran_liaqat_22@sms.edu.pk

ability to incorporate memory and hereditary effects, since fractional operators depend on the entire past evolution of a process rather than only its present state. This feature enables a smooth transition between classical behavior and more complex dynamics, such as slow or fast diffusion, or intermediate responses between purely elastic and purely viscous materials. Owing to these advantages, fractional calculus has found broad applications in viscoelastic material analysis, anomalous diffusion in porous media, electrical circuits with non-ideal capacitive elements, biological and epidemiological models influenced by historical interactions, financial systems with long-memory properties, and modern control systems that require enhanced stability and precision. These features make fractional calculus a realistic and effective framework for modeling natural and engineered systems where classical integer order models fail to capture observed behavior.

Fractional derivatives extend the traditional concept of differentiation to non-integer orders and provide a natural means to describe systems that exhibit memory and long-range dependence. Unlike classical derivatives that depend only on the instantaneous state, fractional derivatives incorporate the entire history of a process, which makes them highly suitable for modeling real phenomena such as viscoelasticity, anomalous diffusion, biological dynamics, and long memory effects in finance and physics. Among the various definitions of fractional derivatives, the Caputo fractional derivative is particularly favored in applied sciences because it accommodates classical initial conditions expressed in terms of integer order derivatives, which leads to mathematically consistent and physically meaningful formulations. The Caputo operator also avoids certain singular behaviors present in other definitions and yields smoother and more realistic solutions for fractional differential equations. These advantages make the Caputo fractional derivative a practical and powerful tool for modeling complex systems where classical integer order frameworks are insufficient.

Numerous academics and scientists are interested in fractional differential equations (FDEs). In the mathematical framework of physical issues, such as those in technology, healthcare, financial markets, and decision theory, the FDEs are widely employed due to their logical underpinnings. Consequently, the FDEs offer important and practical solutions. Approximate analytical methods offer a strong tool for solving FDEs under specified initial or boundary conditions. Several approximate analytical methods, including the operational matrix Bhrawy and Alofi (2013) [2], the Haar wavelet collocation Shiralashetti and Deshi (2016) [12], the differential transforms Maitama and Zhao (2020) [10], the fractional reproducing kernel Hasan et al. (2020) [4], the Aboodh decomposition method Liaqat et al. (2022) [8], and the natural transform homotopy perturbation Jassim and Mohammed (2021) [5], have been described in recent years for solving FDEs.

The technique we recommend is the LRPSM, which combines the RPSM and the Laplace transform (L-T). The given equation is converted into the L-T space to determine the set of rules for our approach. Consequently, we have an algebraic form in L-T space. In the second phase, the new fractional power series in L-T is used to express the algebraic equation solution that was found in the first step in the L-T space. The coefficients of this expansion are found using residual functions and the limit notion. Consequently, we solved the problem at its original place in space by finding the inverse L-T.

The following class of fractional gas dynamics equation (FGDE) is used in this study [3, 13]:

$$\mathcal{D}_t^p F(x,t) = -F(x,t)\mathcal{D}_x F(x,t) + \mathbb{G}F(x,t)(1-F(x,t)) + B(x,t), \tag{1}$$

with the initial condition:

$$F(x,0) = \mathbb{A}(x), \tag{2}$$

where $x \geq 0$, $0 < p \leq 1$, $\mathbb{G}$ is an appropriate constant and $B(x,t)$ represent the basis term. Several branches of natural science, including quantum optics, theoretical biology, circuit theory,

chemical physics, solid-state physics, and others, employ the fractional Fokker-Planck equation (FFPE). It was initially designed to demonstrate Brownian motion by Fokker and Planck [9]. The FFPE uses the general system listed below [15]:

$$\mathcal{D}_t^p F(x,t) = (-\mathcal{D}_x W(x) + \mathcal{D}_{xx} Z(x))F(x,t), \tag{3}$$

with the initial condition:

$$F(x,0) = H(x), \quad x \in \mathbb{R}, \tag{4}$$

where $Z(x) > 0$ is the diffusion factor and $W(x) > 0$ is the drift factor.

The Swift-Hohenberg equation (SHE) has a wide range of applications in engineering and science, including laser studies, biology, physics, hydrodynamics, and fluid dynamics. The SHE is critical to the concept of pattern generation in fluid layers constrained by horizontal well-conducting barriers. The modeling of pattern formation and its various challenges, including pattern selection, noise effects on bifurcations, defect dynamics, and spatiotemporal chaos, makes extensive use of this equation [1]. The generic form of SHE is given by [11]:

$$\frac{\partial}{\partial t} F(x,t) = \mathbb{Q}F(x,t) - (1+\nabla^2)^2 F(x,t) - F^3(x,t), \tag{5}$$

where $x \in \mathbb{R}$, $t > 0$ and $\mathbb{Q}$ is bifurcation parameter, $F(x,t)$ is a scalar function of x and t defined on the line or the plane.

We employed a coupling algorithm that combines L-T and RPSM to extract both approximate solutions (App-S) and exact solutions for FGDE, FFPE, and SHE concerning Caputo fractional derivative (CFD). To validate the accuracy of the App-S derived from LRPSM for nonlinear problems, we measured relative error (Rel-E), absolute error (Abs-E), and residual error (Res-E). Our findings indicate that our method serves as an effective alternative tool for solving fractional nonlinear models.

The organization of the remaining sections is as follows: Section 2 discusses the fundamental concepts utilized in this research study. Section 3 presents applications of the algorithm. Section 4 evaluates the proposed approach based on graphical and numerical results. Finally, Section 5 contains the conclusion.

2 Fundamental Concepts

This section examines the common definitions, characteristics, and implications we employed throughout this study.

Definition 2.1 ([14]). The L-T is a fundamental integral transform widely used in mathematics, physics, engineering, and applied sciences, particularly for solving differential and integral equations.

We examine the functions in a set $\mathbb{Q}$, which is described as

$$\mathbb{Q} = \left\{ \mathcal{F}(t) \;\middle|\; \exists\, P, g_1, g_2 > 0,\ |\mathcal{F}(t)| < P e^{\frac{|t|}{g_i}},\ \text{if } t \in (-1)^i \times [0,\infty) \right\}. \tag{6}$$

The L-T is formulated as

$$\mathcal{L}_p[\mathcal{F}(t)] = \mathcal{B}(q) = \int_0^\infty \mathcal{F}(t) e^{-qt}\, dt, \qquad g_1 \le q \le g_2. \tag{7}$$

Definition 2.2 ([6]). Assume that $\mathcal{F}(t)$ satisfies the axioms of existence of the L-T. Then we have

$$\mathcal{B}(x,q) = \sum_{i=0}^{\infty} \frac{u_i(x)}{q^{ip+1}}. \tag{8}$$

Lemma 2.3. *[[6]] Assume that $\mathcal{F}_1(x,t)$ and $\mathcal{F}_2(x,t)$ satisfy the axioms of existence of the L-T. Let*

$$\mathcal{L}_p[\mathcal{F}_1(x,t)] = \mathcal{B}_1(x,q), \qquad \mathcal{L}_p[\mathcal{F}_2(x,t)] = \mathcal{B}_2(x,q),$$

and let C_1, C_2 be constants. Then the following axioms hold:

(a)

$$\mathcal{L}_p[C_1\mathcal{F}_1(x,t) + C_2\mathcal{F}_2(x,t)] = C_1\mathcal{B}_1(x,q) + C_2\mathcal{B}_2(x,q).$$

(b)

$$\mathcal{L}_p^{-1}[C_1\mathcal{B}_1(x,q) + C_2\mathcal{B}_2(x,q)] = C_1\mathcal{F}_1(x,t) + C_2\mathcal{F}_2(x,t).$$

(c)

$$u_0(x) = \lim_{q\to\infty}(q^p\mathcal{B}(x,q)) = u_0.$$

(d)

$$\mathcal{L}_p\left[{}^{C}D_t^p\mathcal{F}(x,t)\right] = q^p\mathcal{B}(x,q) - \sum_{i=0}^{s-1} q^{p-2-i}D_t^{(i)}\mathcal{F}(x,0), \qquad s-1 < p \le s.$$

Theorem 2.4 ([6]). *Let*

$$\mathcal{L}_p[\mathcal{F}(x,t)] = \mathcal{B}(x,q)$$

be represented as the novel form of a fractional power series

$$\mathcal{B}(x,q) = \sum_{i=0}^{\infty}\frac{\mathcal{U}_i(x)}{q^{ip+2}}.$$

If the following condition holds

$$\left|\partial_x\mathcal{L}_p\left[D_t^{(i+1)p}\mathcal{F}(x,t)\right]\right| \le \mathcal{M},$$

then the remainder $\mathcal{R}_i(x,q)$ of the novel form of power series satisfies

$$|\mathcal{R}_i(x,q)| \le \frac{\mathcal{M}}{q^{(i+1)p+1}}.$$

Theorem 2.5 ([7]). *The L-T of $\mathcal{F}(x,t)$ is*

$$\mathcal{L}_p[\mathcal{F}(x,t)] = \mathcal{B}(x,q),$$

and the fractional power series is given by

$$\mathcal{B}(x,q) = \sum_{i=0}^{\infty}\frac{\mathcal{U}_i(x)}{q^{ip+1}},$$

then we have

$$\mathcal{U}_i(x) = D_t^{ip}\mathcal{F}(x,0),$$

where $i = 0,1,2,\ldots$, and

$$D_t^{ip} = D_t^p \cdot D_t^p \cdot D_t^p \cdots D_t^p \quad (i\text{-times}).$$

Some properties of CFD we have

(a)

$$D_t^{p_1}D_t^{p_2}\mathcal{F}(x,t) = D_t^{p_1+p_2}\mathcal{F}(x,t).$$

(b)

$$D_t^p C = 0, \qquad C \in \mathbb{R}.$$

(c)

$$D_t^p (t-\eta)^c = \frac{\Gamma(c+1)}{\Gamma(c+1-p)}(t-\eta)^{c-p}, \qquad i-1 < p \le i,\ c > i-1,\ c \in \mathbb{N},\ c \in \mathbb{R}.$$

(d)

$$D_t^p \left[C_1 \mathcal{F}_1(x,t) + C_2 \mathcal{F}_2(x,t)\right] = C_1 D_t^p \mathcal{F}_1(x,t) + C_2 D_t^p \mathcal{F}_2(x,t), \qquad C_1, C_2 \in \mathbb{R}.$$

(e)

$$D_t^p \left[J_t^p \mathcal{F}(x,t)\right] = \mathcal{F}(x,t),$$

where J_t^p is the Riemann–Liouville integral of order p.

3 The Algorithm of LRPSM

The following steps outline the fundamental algorithm of the proposed approach for solving Eq. (9). By applying the L-T together with the RPSM, the general analytical solution of nonlinear partial differential equations (PDEs) in standard operator form is obtained.

Consider the time-fractional nonlinear PDE:

$$\mathcal{D}_t^p F(x,t) + \mathcal{L}(F(x,t)) + \mathcal{N}(F(x,t)) = \mathcal{R}(x,t) \tag{9}$$

with the initial condition:

$$F(x,0) = \mathcal{G}(x), \tag{10}$$

where $x > 0, t > 0, 0 < p \le 1$, $\mathcal{D}_t^p$ is the CFD of $F(x,t)$, $\mathcal{L}(F(x,t))$ stands for a linear differential operator, $\mathcal{N}(F(x,t))$ for one that is nonlinear, $\mathcal{R}(x,t)$ for a specified term and $\mathcal{G}(x)$ for the function of x.

Step 1. Applying L-T to Eq. (9), using the linear property of L-T and Lemma 2.3(d), and making some calculations, we get

$$\begin{aligned}\mathfrak{B}(x,q) = &-\frac{1}{q^p}\mathfrak{L}_p[\mathcal{L}(\mathfrak{B}(x,q))] - \frac{1}{q^p}\mathfrak{L}_p[\mathcal{N}(\mathfrak{B}(x,q))] \\ &+ \frac{1}{q}\mathcal{G}(x) + \frac{1}{q^p}\mathcal{H}(x,q),\end{aligned} \tag{11}$$

where $\mathfrak{L}_p[F(x,t)] = \mathfrak{B}(x,q)$ and $\mathfrak{L}_p[\mathcal{R}(x,t)] = \mathcal{H}(x,q)$.

Step 2. Consider the solution of Eq. (11), which has the following form:

$$\mathfrak{B}(x,q) = \sum_{i=0}^{\infty} \frac{\mathfrak{U}_i(x)}{q^{ip+1}}. \tag{12}$$

Step 3. Obtain the kth-truncated series

$$\mathfrak{B}_k(x,q) = \sum_{i=0}^{k} \frac{\mathfrak{U}_i(x)}{q^{ip+1}}. \tag{13}$$

Step 4. By using Lemma 2.3(c), we have the following

$$\mathfrak{U}_0(x) = \lim_{q\to\infty} (q\mathfrak{B}(x,q)) = \mathcal{G}(x). \tag{14}$$

The kth-truncated series becomes

$$\mathfrak{B}_k(x,q) = \frac{1}{q}\mathcal{G}(x) + \sum_{i=1}^{k} \frac{\mathfrak{U}_i(x)}{q^{ip+1}}. \tag{15}$$

Step 5. The L-T residual function (LRF) and kth LRF are

$$\begin{aligned}\mathfrak{LRES}(x,q) = \mathfrak{B}(x,q) + \frac{1}{q^p}\mathfrak{L}_p[\mathcal{L}(\mathfrak{B}(x,q))] + \frac{1}{q^p}\mathfrak{L}_p[\mathcal{N}(\mathfrak{B}(x,q))] \\ - \frac{1}{q}\mathcal{G}(x) - \frac{1}{q^p}\mathcal{H}(x,q),\end{aligned} \tag{16}$$

$$\begin{aligned}\mathfrak{LRES}_k(x,q) = \mathfrak{B}_k(x,q) + \frac{1}{q^p}\mathfrak{L}_p[\mathcal{L}(\mathfrak{B}_k(x,q))] + \frac{1}{q^p}\mathfrak{L}_p[\mathcal{N}(\mathfrak{B}_k(x,q))] \\ - \frac{1}{q}\mathcal{G}(x) - \frac{1}{q^p}\mathcal{H}(x,q).\end{aligned} \tag{17}$$

Step 6. Solve the following equation for $\mathfrak{U}_i(x)$

$$\lim_{q\to\infty} \left(q^{kp+1}\mathfrak{LRES}_k(x,q)\right) = 0. \tag{18}$$

Step 7. Replace the obtained values of $\mathfrak{U}_k(x)$ into kth-truncated series of $\mathfrak{B}_k(x,q)$ to derive the kth-approximate solution of Eq. (11).

Step 8. Use the inverse L-T on $\mathfrak{B}_k(x,q)$ to obtain the kth-approximate solution $F_k(x,t)$.

4 Applications of the LRPSM

Five nonlinear problems are solved in this section to assess the effectiveness of the LRPSM.

Problem 1. Consider the non-linear and time FGDE that follows:

$$\mathcal{D}_t^p F(x,t) + F(x,t)\mathcal{D}_x F(x,t) - F(x,t)(1 - F(x,t)) = 0, \tag{19}$$

where $t \geq 0, 0 \leq x \leq 1, 0 < p \leq 1$, with the initial condition:

$$F(x,0) = e^{-x}. \tag{20}$$

Applying the L-T to Eq. (19) and using the procedure explained in Section 3, we have

$$\begin{aligned}\mathfrak{B}(x,q) = \frac{1}{q}e^{-x} - \frac{1}{q^p}\mathfrak{L}_p\left[\mathfrak{L}_p^{-1}[\mathfrak{B}(x,q)]\cdot\mathcal{D}_x\mathfrak{L}_p^{-1}[\mathfrak{B}(x,q)]\right] \\ - \frac{1}{q^p}\mathfrak{L}_p\left[\mathfrak{L}_p^{-1}[\mathfrak{B}(x,q)]\right] + \frac{1}{q^p}\mathfrak{L}_p\left[\mathfrak{L}_p^{-1}[\mathfrak{B}(x,q)]\right]^2 = 0,\end{aligned} \tag{21}$$

where $\mathfrak{L}_p[F(x,t)] = \mathfrak{B}(x,q)$ and $F(x,t) = \mathfrak{L}_p^{-1}[\mathfrak{B}(x,q)]$.

By using Lemma 2.3(c), we get

$$\mathfrak{U}_0(x) = \lim_{q\to\infty} (q\mathfrak{B}(x,q)) = F(x,0) = e^{-x}. \tag{22}$$

The LRF is defined as

$$\begin{aligned}\mathfrak{LRES}(x,q) = \mathfrak{B}(x,q) - \frac{1}{q}e^{-x} \\ - \frac{1}{q^p}\mathfrak{L}_p\left[\mathfrak{L}_p^{-1}[\mathfrak{B}(x,q)]\cdot \mathcal{D}_x\mathfrak{L}_p^{-1}[\mathfrak{B}(x,q)]\right] \\ - \frac{1}{q^p}\mathfrak{L}_p\left[\mathfrak{L}_p^{-1}[\mathfrak{B}(x,q)]\right] + \frac{1}{q^p}\mathfrak{L}_p\left[\mathfrak{L}_p^{-1}[\mathfrak{B}(x,q)]\right]^2.\end{aligned} \tag{23}$$

The kth-truncated LRF takes the following form:

$$\begin{aligned}\mathfrak{LRES}_k(x,q) = \mathfrak{B}_k(x,q) - \frac{1}{q}e^{-x} \\ - \frac{1}{q^p}\mathfrak{L}_p\left[\mathfrak{L}_p^{-1}[\mathfrak{B}_k(x,q)]\cdot \mathcal{D}_x\mathfrak{L}_p^{-1}[\mathfrak{B}_k(x,q)]\right] \\ - \frac{1}{q^p}\mathfrak{L}_p\left[\mathfrak{L}_p^{-1}[\mathfrak{B}_k(x,q)]\right] + \frac{1}{q^p}\mathfrak{L}_p\left[\mathfrak{L}_p^{-1}[\mathfrak{B}_k(x,q)]\right]^2.\end{aligned} \tag{24}$$

Now, we construct the kth-truncated series solution in Laplace space:

$$\mathfrak{B}_k(x,q) = \frac{e^{-x}}{q} + \sum_{i=1}^{k}\frac{\mathfrak{U}_i(x)}{q^{ip+1}}. \tag{25}$$

To determine the coefficients $\mathfrak{U}_i(x)$, we solve the following equation:

$$\lim_{q\to\infty}\left(q^{kp+1}\mathfrak{LRES}_k(x,q)\right) = 0. \tag{26}$$

For $k = 1$, the first truncated series is:

$$\mathfrak{B}_1(x,q) = \frac{e^{-x}}{q} + \frac{\mathfrak{U}_1(x)}{q^{p+1}}. \tag{27}$$

Substituting into the first LRF and using Eq. (26) with $k = 1$, we get:

$$\mathfrak{U}_1(x) = \frac{e^{-x}}{q^{p+1}}. \tag{28}$$

For $k = 2$, the second truncated series is:

$$\mathfrak{B}_2(x,q) = \frac{e^{-x}}{q} + \frac{e^{-x}}{q^{p+1}} + \frac{\mathfrak{U}_2(x)}{q^{2p+1}}. \tag{29}$$

Solving $\lim_{q\to\infty}\left(q^{2p+1}\mathfrak{LRES}_2(x,q)\right) = 0$, we obtain:

$$\mathfrak{U}_2(x) = \frac{e^{-x}}{q^{2p+1}}. \tag{30}$$

Continuing this process, we obtain the following coefficients:

$$\mathfrak{U}_3(x) = \frac{e^{-x}}{q^{3p+1}}, \tag{31}$$

$$\mathfrak{U}_4(x) = \frac{e^{-x}}{q^{4p+1}}, \tag{32}$$

$$\mathfrak{U}_5(x) = \frac{e^{-x}}{q^{5p+1}}. \tag{33}$$

In this way, the expansion-form solution of Eq. (19) in Laplace space is provided as

$$\begin{aligned}\mathfrak{B}(x,q) = &\frac{e^{-x}}{q} + \frac{e^{-x}}{q^{p+1}} + \frac{e^{-x}}{q^{2p+1}} + \frac{e^{-x}}{q^{3p+1}} \\ &+ \frac{e^{-x}}{q^{4p+1}} + \frac{e^{-x}}{q^{5p+1}} + \cdots .\end{aligned} \tag{34}$$

By using the inverse L-T, we get an expansion solution in the original space:

$$\begin{aligned}F(x,t) = e^{-x} + e^{-x}\frac{t^p}{\Gamma(p+1)} + e^{-x}\frac{t^{2p}}{\Gamma(2p+1)} + e^{-x}\frac{t^{3p}}{\Gamma(3p+1)} \\ + e^{-x}\frac{t^{4p}}{\Gamma(4p+1)} + e^{-x}\frac{t^{5p}}{\Gamma(5p+1)} + \cdots .\end{aligned} \tag{35}$$

The exact solution of Eq. (19) becomes as follows:

$$F(x,t) = e^{-x}\mathbb{E}_p(t), \tag{36}$$

where $\mathbb{E}_p(t) = \sum_{n=0}^{\infty} \frac{t^{np}}{\Gamma(np+1)}$ is the Mittag-Leffler function.

Remark 4.1. For the special case when $p = 1$, the Mittag-Leffler function reduces to the exponential function, and the solution becomes $F(x,t) = e^{-x}e^{t} = e^{t-x}$, which is the exact solution of the classical (integer-order) gas dynamics equation.

Problem 2. Consider the non-linear and time FGDE that follows:

$$\mathcal{D}_t^p F(x,t) + F(x,t)\mathcal{D}_x F(x,t) - F(x,t)\log \mathfrak{u} - F^2(x,t)\log \mathfrak{u} = 0, \tag{37}$$

where $t \geq 0$, $0 \leq x \leq 1$, $0 < p \leq 1$, with the initial condition:

$$F(x,0) = \mathfrak{u}^{-x}. \tag{38}$$

Applying the L-T to Eq. (37) and using the procedure explained in Section 3, we have

$$\begin{aligned}\mathfrak{B}(x,q) = &\frac{1}{q}\mathfrak{u}^{-x} - \frac{1}{q^p}\mathfrak{L}_p\left[\mathfrak{L}_p^{-1}[\mathfrak{B}(x,q)]\cdot\mathcal{D}_x\mathfrak{L}_p^{-1}[\mathfrak{B}(x,q)]\right] \\ &- \frac{1}{q^p}\mathfrak{L}_p\left[\mathfrak{L}_p^{-1}[\mathfrak{B}(x,q)]\right]\log \mathfrak{u} \\ &+ \frac{1}{q^p}\mathfrak{L}_p\left[\mathfrak{L}_p^{-1}[\mathfrak{B}(x,q)]\right]^2\log \mathfrak{u},\end{aligned} \tag{39}$$

where $\mathfrak{L}_p[F(x,t)] = \mathfrak{B}(x,q)$ and $F(x,t) = \mathfrak{L}_p^{-1}[\mathfrak{B}(x,q)]$.

By using Lemma 2.3(c), we get

$$\mathfrak{U}_0(x) = \lim_{q\to\infty}(q\mathfrak{B}(x,q)) = F(x,0) = \mathfrak{u}^{-x}. \tag{40}$$

The LRF is defined as

$$\begin{aligned}\mathcal{LRES}(x,q) = \mathfrak{B}(x,q) &- \frac{1}{q}\mathfrak{u}^{-x} \\ &- \frac{1}{q^p}\mathfrak{L}_p\left[\mathfrak{L}_p^{-1}[\mathfrak{B}(x,q)]\cdot\mathcal{D}_x\mathfrak{L}_p^{-1}[\mathfrak{B}(x,q)]\right] \\ &- \frac{1}{q^p}\mathfrak{L}_p\left[\mathfrak{L}_p^{-1}[\mathfrak{B}(x,q)]\right]\log \mathfrak{u} \\ &+ \frac{1}{q^p}\mathfrak{L}_p\left[\mathfrak{L}_p^{-1}[\mathfrak{B}(x,q)]\right]^2\log \mathfrak{u}.\end{aligned} \tag{41}$$

The kth-truncated LRF takes the following form:

$$\begin{aligned}\mathfrak{LRES}_k(x,q) = \mathfrak{B}_k(x,q) &- \frac{1}{q}\mathfrak{u}^{-x} \\ &- \frac{1}{q^p}\mathfrak{L}_p\left[\mathfrak{L}_p^{-1}[\mathfrak{B}_k(x,q)]\cdot \mathcal{D}_x\mathfrak{L}_p^{-1}[\mathfrak{B}_k(x,q)]\right] \\ &- \frac{1}{q^p}\mathfrak{L}_p\left[\mathfrak{L}_p^{-1}[\mathfrak{B}_k(x,q)]\right]\log\mathfrak{u} \\ &+ \frac{1}{q^p}\mathfrak{L}_p\left[\mathfrak{L}_p^{-1}[\mathfrak{B}_k(x,q)]\right]^2\log\mathfrak{u}.\end{aligned} \tag{42}$$

Now, we construct the kth-truncated series solution in Laplace space:

$$\mathfrak{B}_k(x,q) = \frac{\mathfrak{u}^{-x}}{q} + \sum_{i=1}^{k}\frac{\mathfrak{U}_i(x)}{q^{ip+1}}. \tag{43}$$

To determine the coefficients $\mathfrak{U}_i(x)$, we solve the following equation:

$$\lim_{q\to\infty}\left(q^{kp+1}\mathfrak{LRES}_k(x,q)\right) = 0. \tag{44}$$

For $k = 1$, the first truncated series is:

$$\mathfrak{B}_1(x,q) = \frac{\mathfrak{u}^{-x}}{q} + \frac{\mathfrak{U}_1(x)}{q^{p+1}}. \tag{45}$$

Substituting into the first LRF and using Eq. (44) with $k = 1$, we get:

$$\mathfrak{U}_1(x) = \mathfrak{u}^{-x}\frac{\log\mathfrak{u}}{q^{p+1}}. \tag{46}$$

For $k = 2$, the second truncated series is:

$$\mathfrak{B}_2(x,q) = \frac{\mathfrak{u}^{-x}}{q} + \frac{\mathfrak{u}^{-x}\log\mathfrak{u}}{q^{p+1}} + \frac{\mathfrak{U}_2(x)}{q^{2p+1}}. \tag{47}$$

Solving $\lim_{q\to\infty}\left(q^{2p+1}\mathfrak{LRES}_2(x,q)\right) = 0$, we obtain:

$$\mathfrak{U}_2(x) = \mathfrak{u}^{-x}\frac{(\log\mathfrak{u})^2}{q^{2p+1}}. \tag{48}$$

For $k = 3$, the third truncated series is:

$$\mathfrak{B}_3(x,q) = \frac{\mathfrak{u}^{-x}}{q} + \frac{\mathfrak{u}^{-x}\log\mathfrak{u}}{q^{p+1}} + \frac{\mathfrak{u}^{-x}(\log\mathfrak{u})^2}{q^{2p+1}} + \frac{\mathfrak{U}_3(x)}{q^{3p+1}}. \tag{49}$$

Solving $\lim_{q\to\infty}\left(q^{3p+1}\mathfrak{LRES}_3(x,q)\right) = 0$, we obtain:

$$\mathfrak{U}_3(x) = \mathfrak{u}^{-x}\frac{(\log\mathfrak{u})^3}{q^{3p+1}}. \tag{50}$$

Continuing this process, we obtain the following coefficients:

$$\mathfrak{U}_4(x) = \mathfrak{u}^{-x}\frac{(\log \mathfrak{u})^4}{q^{4p+1}}, \tag{51}$$

$$\mathfrak{U}_5(x) = \mathfrak{u}^{-x}\frac{(\log \mathfrak{u})^5}{q^{5p+1}}, \tag{52}$$

$$\mathfrak{U}_6(x) = \mathfrak{u}^{-x}\frac{(\log \mathfrak{u})^6}{q^{6p+1}}, \tag{53}$$

$$\mathfrak{U}_7(x) = \mathfrak{u}^{-x}\frac{(\log \mathfrak{u})^7}{q^{7p+1}}, \tag{54}$$

$$\mathfrak{U}_8(x) = \mathfrak{u}^{-x}\frac{(\log \mathfrak{u})^8}{q^{8p+1}}. \tag{55}$$

In this way, the expansion-form solution of Eq. (37) in Laplace space is provided as

$$\begin{aligned}\mathfrak{B}(x,q) = {} & \frac{\mathfrak{u}^{-x}}{q} + \mathfrak{u}^{-x}\frac{\log \mathfrak{u}}{q^{p+1}} + \mathfrak{u}^{-x}\frac{(\log \mathfrak{u})^2}{q^{2p+1}} + \mathfrak{u}^{-x}\frac{(\log \mathfrak{u})^3}{q^{3p+1}} \\ & + \mathfrak{u}^{-x}\frac{(\log \mathfrak{u})^4}{q^{4p+1}} + \mathfrak{u}^{-x}\frac{(\log \mathfrak{u})^5}{q^{5p+1}} + \mathfrak{u}^{-x}\frac{(\log \mathfrak{u})^6}{q^{6p+1}} \\ & + \mathfrak{u}^{-x}\frac{(\log \mathfrak{u})^7}{q^{7p+1}} + \mathfrak{u}^{-x}\frac{(\log \mathfrak{u})^8}{q^{8p+1}} + \cdots .\end{aligned} \tag{56}$$

By using the inverse L-T, we get an expansion solution in the original space:

$$\begin{aligned}F(x,t) = {} & \mathfrak{u}^{-x} + \mathfrak{u}^{-x}\frac{t^p}{\Gamma(p+1)}\log \mathfrak{u} + \mathfrak{u}^{-x}\frac{t^{2p}}{\Gamma(2p+1)}(\log \mathfrak{u})^2 \\ & + \mathfrak{u}^{-x}\frac{t^{3p}}{\Gamma(3p+1)}(\log \mathfrak{u})^3 + \mathfrak{u}^{-x}\frac{t^{4p}}{\Gamma(4p+1)}(\log \mathfrak{u})^4 \\ & + \mathfrak{u}^{-x}\frac{t^{5p}}{\Gamma(5p+1)}(\log \mathfrak{u})^5 + \mathfrak{u}^{-x}\frac{t^{6p}}{\Gamma(6p+1)}(\log \mathfrak{u})^6 \\ & + \mathfrak{u}^{-x}\frac{t^{7p}}{\Gamma(7p+1)}(\log \mathfrak{u})^7 + \mathfrak{u}^{-x}\frac{t^{8p}}{\Gamma(8p+1)}(\log \mathfrak{u})^8 + \cdots .\end{aligned} \tag{57}$$

The exact solution of Eq. (37) becomes as follows:

$$F(x,t) = \mathfrak{u}^{-x}\mathbb{E}_p(t\log \mathfrak{u}), \tag{58}$$

where $\mathbb{E}_p(z) = \sum_{n=0}^{\infty}\frac{z^n}{\Gamma(np+1)}$ is the Mittag-Leffler function.

Remark 4.2. For the special case when $p = 1$, the Mittag-Leffler function reduces to the exponential function, and the solution becomes $F(x,t) = \mathfrak{u}^{-x}e^{t\log \mathfrak{u}} = \mathfrak{u}^{-x}\mathfrak{u}^t = \mathfrak{u}^{t-x}$, which is the exact solution of the classical (integer-order) gas dynamics equation with logarithmic term.

Problem 3. Consider the following non-linear and time FFPE:

$$\begin{aligned}\mathcal{D}_t^p F(x,t) = {} & \left(-\mathcal{D}_x\left(\frac{\mathcal{S}+r-4}{2}x\right) + \mathcal{D}_{xx}\left(\frac{x^2}{2}\right)\right)F(x,t) \\ & + \left(-\mathcal{D}_x\left(\frac{4}{x}F^2(x,t)\right) + \mathcal{D}_{xx}\left(F^2(x,t)\right)\right),\end{aligned} \tag{59}$$

where $t \geq 0, 0 \leq x \leq 1, 0 < p \leq 1, \mathcal{S}$ and r are constants, with the initial condition:

$$F(x,0) = e^x. \tag{60}$$

Applying the L-T to Eq. (59) and using the procedure explained in Section 3, we have

$$\begin{aligned}
\mathfrak{B}(x,q) = {} & \frac{e^x}{q} + \frac{(\mathcal{S}+r-4)}{2q^p}\left(\mathfrak{B}(x,q) + x\mathcal{D}_x\mathfrak{B}(x,q)\right) \\
& + \frac{1}{2q^p}\left(2\mathfrak{B}(x,q) + 4x\mathcal{D}_x\mathfrak{B}(x,q) + x^2\mathcal{D}_{xx}\mathfrak{B}(x,q)\right) \\
& - \frac{4}{q^p}\left(-\frac{1}{x^2}\mathfrak{L}_p\left[\mathfrak{L}_p^{-1}[\mathfrak{B}(x,q)]\right]^2 + \frac{2}{x}\mathfrak{L}_p\left[\mathfrak{L}_p^{-1}[\mathfrak{B}(x,q)]\cdot\mathcal{D}_x\mathfrak{L}_p^{-1}[\mathfrak{B}(x,q)]\right]\right) \\
& + \frac{1}{q^p}\left(2\mathfrak{L}_p\left[\mathfrak{L}_p^{-1}[\mathfrak{B}(x,q)]\cdot\mathcal{D}_x\mathfrak{L}_p^{-1}[\mathfrak{B}(x,q)]\right]\right. \\
& \left. + 2\mathfrak{L}_p\left[\left(\mathcal{D}_x\mathfrak{L}_p^{-1}[\mathfrak{B}(x,q)]\right)^2\right] + 2\mathfrak{L}_p\left[\mathfrak{L}_p^{-1}[\mathfrak{B}(x,q)]\cdot\mathcal{D}_{xx}\mathfrak{L}_p^{-1}[\mathfrak{B}(x,q)]\right]\right),
\end{aligned} \tag{61}$$

where $\mathfrak{L}_p[F(x,t)] = \mathfrak{B}(x,q)$ and $F(x,t) = \mathfrak{L}_p^{-1}[\mathfrak{B}(x,q)]$.

By using Lemma 2.3(c), we get

$$\mathfrak{U}_0(x) = \lim_{q\to\infty}\left(q\mathfrak{B}(x,q)\right) = F(x,0) = e^x. \tag{62}$$

The LRF is defined as

$$\begin{aligned}
\mathfrak{LRES}(x,q) = {} & \mathfrak{B}(x,q) - \frac{e^x}{q} \\
& - \frac{(\mathcal{S}+r-4)}{2q^p}\left(\mathfrak{B}(x,q) + x\mathcal{D}_x\mathfrak{B}(x,q)\right) \\
& - \frac{1}{2q^p}\left(2\mathfrak{B}(x,q) + 4x\mathcal{D}_x\mathfrak{B}(x,q) + x^2\mathcal{D}_{xx}\mathfrak{B}(x,q)\right) \\
& + \frac{4}{q^p}\left(-\frac{1}{x^2}\mathfrak{L}_p\left[\mathfrak{L}_p^{-1}[\mathfrak{B}(x,q)]\right]^2 + \frac{2}{x}\mathfrak{L}_p\left[\mathfrak{L}_p^{-1}[\mathfrak{B}(x,q)]\cdot\mathcal{D}_x\mathfrak{L}_p^{-1}[\mathfrak{B}(x,q)]\right]\right) \\
& - \frac{1}{q^p}\left(2\mathfrak{L}_p\left[\mathfrak{L}_p^{-1}[\mathfrak{B}(x,q)]\cdot\mathcal{D}_x\mathfrak{L}_p^{-1}[\mathfrak{B}(x,q)]\right]\right. \\
& \left. + 2\mathfrak{L}_p\left[\left(\mathcal{D}_x\mathfrak{L}_p^{-1}[\mathfrak{B}(x,q)]\right)^2\right] + 2\mathfrak{L}_p\left[\mathfrak{L}_p^{-1}[\mathfrak{B}(x,q)]\cdot\mathcal{D}_{xx}\mathfrak{L}_p^{-1}[\mathfrak{B}(x,q)]\right]\right).
\end{aligned} \tag{63}$$

The kth-truncated LRF takes the following form:

$$\begin{aligned}
\mathfrak{LRES}_k(x,q) = {} & \mathfrak{B}_k(x,q) - \frac{e^x}{q} \\
& - \frac{(\mathcal{S}+r-4)}{2q^p}\left(\mathfrak{B}_k(x,q) + x\mathcal{D}_x\mathfrak{B}_k(x,q)\right) \\
& - \frac{1}{2q^p}\left(2\mathfrak{B}_k(x,q) + 4x\mathcal{D}_x\mathfrak{B}_k(x,q) + x^2\mathcal{D}_{xx}\mathfrak{B}_k(x,q)\right) \\
& + \frac{4}{q^p}\left(-\frac{1}{x^2}\mathfrak{L}_p\left[\mathfrak{L}_p^{-1}[\mathfrak{B}_k(x,q)]\right]^2 + \frac{2}{x}\mathfrak{L}_p\left[\mathfrak{L}_p^{-1}[\mathfrak{B}_k(x,q)]\cdot\mathcal{D}_x\mathfrak{L}_p^{-1}[\mathfrak{B}_k(x,q)]\right]\right) \\
& - \frac{1}{q^p}\left(2\mathfrak{L}_p\left[\mathfrak{L}_p^{-1}[\mathfrak{B}_k(x,q)]\cdot\mathcal{D}_x\mathfrak{L}_p^{-1}[\mathfrak{B}_k(x,q)]\right]\right. \\
& \left. + 2\mathfrak{L}_p\left[\left(\mathcal{D}_x\mathfrak{L}_p^{-1}[\mathfrak{B}_k(x,q)]\right)^2\right] + 2\mathfrak{L}_p\left[\mathfrak{L}_p^{-1}[\mathfrak{B}_k(x,q)]\cdot\mathcal{D}_{xx}\mathfrak{L}_p^{-1}[\mathfrak{B}_k(x,q)]\right]\right).
\end{aligned} \tag{64}$$

Now, we construct the kth-truncated series solution in Laplace space:

$$\mathfrak{B}_k(x,q) = \frac{e^x}{q} + \sum_{i=1}^{k} \frac{\mathfrak{U}_i(x)}{q^{ip+1}}. \tag{65}$$

To determine the coefficients $\mathfrak{U}_i(x)$, we solve the following equation:

$$\lim_{q\to\infty} \left(q^{kp+1} \mathfrak{LRES}_k(x,q) \right) = 0. \tag{66}$$

For $k = 1$, the first truncated series is:

$$\mathfrak{B}_1(x,q) = \frac{e^x}{q} + \frac{\mathfrak{U}_1(x)}{q^{p+1}}. \tag{67}$$

Substituting into the first LRF and using Eq. (66) with $k = 1$, we get:

$$\mathfrak{U}_1(x) = e^x \frac{(\mathcal{S} + r - 4)}{q^{p+1}}. \tag{68}$$

For $k = 2$, the second truncated series is:

$$\mathfrak{B}_2(x,q) = \frac{e^x}{q} + \frac{e^x(\mathcal{S} + r - 4)}{q^{p+1}} + \frac{\mathfrak{U}_2(x)}{q^{2p+1}}. \tag{69}$$

Solving $\lim_{q\to\infty} \left(q^{2p+1} \mathfrak{LRES}_2(x,q) \right) = 0$, we obtain:

$$\mathfrak{U}_2(x) = e^x \frac{(\mathcal{S} + r - 4)^2}{q^{2p+1}}. \tag{70}$$

For $k = 3$, the third truncated series is:

$$\mathfrak{B}_3(x,q) = \frac{e^x}{q} + \frac{e^x(\mathcal{S} + r - 4)}{q^{p+1}} + \frac{e^x(\mathcal{S} + r - 4)^2}{q^{2p+1}} + \frac{\mathfrak{U}_3(x)}{q^{3p+1}}. \tag{71}$$

Solving $\lim_{q\to\infty} \left(q^{3p+1} \mathfrak{LRES}_3(x,q) \right) = 0$, we obtain:

$$\mathfrak{U}_3(x) = e^x \frac{(\mathcal{S} + r - 4)^3}{q^{3p+1}}. \tag{72}$$

For $k = 4$, the fourth truncated series is:

$$\mathfrak{B}_4(x,q) = \frac{e^x}{q} + \frac{e^x(\mathcal{S} + r - 4)}{q^{p+1}} + \frac{e^x(\mathcal{S} + r - 4)^2}{q^{2p+1}} + \frac{e^x(\mathcal{S} + r - 4)^3}{q^{3p+1}} + \frac{\mathfrak{U}_4(x)}{q^{4p+1}}. \tag{73}$$

Solving $\lim_{q\to\infty} \left(q^{4p+1} \mathfrak{LRES}_4(x,q) \right) = 0$, we obtain:

$$\mathfrak{U}_4(x) = e^x \frac{(\mathcal{S} + r - 4)^4}{q^{4p+1}}. \tag{74}$$

For $k = 5$, the fifth truncated series is:

$$\mathfrak{B}_5(x,q) = \frac{e^x}{q} + \frac{e^x(\mathcal{S} + r - 4)}{q^{p+1}} + \frac{e^x(\mathcal{S} + r - 4)^2}{q^{2p+1}} + \frac{e^x(\mathcal{S} + r - 4)^3}{q^{3p+1}} + \frac{e^x(\mathcal{S} + r - 4)^4}{q^{4p+1}} + \frac{\mathfrak{U}_5(x)}{q^{5p+1}}. \tag{75}$$

Solving $\lim_{q\to\infty}\left(q^{5p+1}\mathfrak{LRES}_5(x,q)\right)=0$, we obtain:

$$\mathfrak{U}_5(x)=e^x\frac{(\mathcal{S}+r-4)^5}{q^{5p+1}}. \tag{76}$$

In this way, the expansion-form solution of Eq. (59) in Laplace space is provided as

$$\begin{aligned}\mathfrak{B}(x,q)=&\frac{e^x}{q}+e^x\frac{(\mathcal{S}+r-4)}{q^{p+1}}+e^x\frac{(\mathcal{S}+r-4)^2}{q^{2p+1}}+e^x\frac{(\mathcal{S}+r-4)^3}{q^{3p+1}}\\&+e^x\frac{(\mathcal{S}+r-4)^4}{q^{4p+1}}+e^x\frac{(\mathcal{S}+r-4)^5}{q^{5p+1}}+\cdots.\end{aligned} \tag{77}$$

By using the inverse L-T, we get an expansion solution in the original space:

$$\begin{aligned}F(x,t)=&e^x+e^x\frac{t^p}{\Gamma(p+1)}(\mathcal{S}+r-4)+e^x\frac{t^{2p}}{\Gamma(2p+1)}(\mathcal{S}+r-4)^2\\&+e^x\frac{t^{3p}}{\Gamma(3p+1)}(\mathcal{S}+r-4)^3+e^x\frac{t^{4p}}{\Gamma(4p+1)}(\mathcal{S}+r-4)^4\\&+e^x\frac{t^{5p}}{\Gamma(5p+1)}(\mathcal{S}+r-4)^5+\cdots.\end{aligned} \tag{78}$$

The exact solution of Eq. (59) becomes as follows:

$$F(x,t)=e^x\mathbb{E}_p\left(t(\mathcal{S}+r-4)\right), \tag{79}$$

where $\mathbb{E}_p(z)=\sum_{n=0}^{\infty}\frac{z^n}{\Gamma(np+1)}$ is the Mittag-Leffler function.

Remark 4.3. For the special case when $p=1$, the Mittag-Leffler function reduces to the exponential function, and the solution becomes $F(x,t)=e^xe^{t(\mathcal{S}+r-4)}=e^{x+t(\mathcal{S}+r-4)}$, which is the exact solution of the classical (integer-order) Fokker-Planck equation.

Problem 4. The following non-linear, time-fractional SHE is considered:

$$\begin{aligned}&\mathcal{D}_t^pF(x,t)+(1-r)F(x,t)+2\mathcal{D}_{xx}F(x,t)+\mathcal{D}_{xxxx}F(x,t)\\&\quad-F^2(x,t)+\left(\mathcal{D}_xF(x,t)\right)^2=0,\quad 0<p\leq 1,\end{aligned} \tag{80}$$

with the initial condition:

$$F(x,0)=e^x. \tag{81}$$

Applying the L-T to Eq. (80) and using the procedure explained in Section 3, we have

$$\begin{aligned}\mathfrak{B}(x,q)=&\frac{1}{q}e^x-(1-r)\frac{1}{q^p}\mathfrak{B}(x,q)-2\frac{1}{q^p}\mathcal{D}_{xx}\mathfrak{B}(x,q)-\frac{1}{q^p}\mathcal{D}_{xxxx}\mathfrak{B}(x,q)\\&+\frac{1}{q^p}\mathfrak{L}_p\left[\mathfrak{L}_p^{-1}[\mathfrak{B}(x,q)]\right]^2-\frac{1}{q^p}\mathfrak{L}_p\left(\mathcal{D}_x\mathfrak{L}_p^{-1}[\mathfrak{B}(x,q)]\right)^2,\end{aligned} \tag{82}$$

where $\mathfrak{L}_p[F(x,t)]=\mathfrak{B}(x,q)$ and $F(x,t)=\mathfrak{L}_p^{-1}[\mathfrak{B}(x,q)]$.

By using Lemma 2.3(c), we get

$$\mathfrak{U}_0(x)=\lim_{q\to\infty}\left(q\mathfrak{B}(x,q)\right)=F(x,0)=e^x. \tag{83}$$

The LRF is defined as

$$\begin{aligned}\mathcal{LRES}(x,q) &= \mathfrak{B}(x,q) - \frac{1}{q}e^x + (1-r)\frac{1}{q^p}\mathfrak{B}(x,q) + 2\frac{1}{q^p}\mathcal{D}_{xx}\mathfrak{B}(x,q)\\ &+ \frac{1}{q^p}\mathcal{D}_{xxxx}\mathfrak{B}(x,q) - \frac{1}{q^p}\mathfrak{L}_p\left[\mathfrak{L}_p^{-1}[\mathfrak{B}(x,q)]\right]^2\\ &+ \frac{1}{q^p}\mathfrak{L}_p\left(\mathcal{D}_x\mathfrak{L}_p^{-1}[\mathfrak{B}(x,q)]\right)^2.\end{aligned} \tag{84}$$

The kth-truncated LRF takes the following form:

$$\begin{aligned}\mathcal{LRES}_k(x,q) &= \mathfrak{B}_k(x,q) - \frac{1}{q}e^x + (1-r)\frac{1}{q^p}\mathfrak{B}_k(x,q) + 2\frac{1}{q^p}\mathcal{D}_{xx}\mathfrak{B}_k(x,q)\\ &+ \frac{1}{q^p}\mathcal{D}_{xxxx}\mathfrak{B}_k(x,q) - \frac{1}{q^p}\mathfrak{L}_p\left[\mathfrak{L}_p^{-1}[\mathfrak{B}_k(x,q)]\right]^2\\ &+ \frac{1}{q^p}\mathfrak{L}_p\left(\mathcal{D}_x\mathfrak{L}_p^{-1}[\mathfrak{B}_k(x,q)]\right)^2.\end{aligned} \tag{85}$$

Now, we construct the kth-truncated series solution in Laplace space:

$$\mathfrak{B}_k(x,q) = \frac{e^x}{q} + \sum_{i=1}^{k}\frac{\mathfrak{U}_i(x)}{q^{ip+1}}. \tag{86}$$

To determine the coefficients $\mathfrak{U}_i(x)$, we solve the following equation:

$$\lim_{q\to\infty}\left(q^{kp+1}\mathcal{LRES}_k(x,q)\right) = 0. \tag{87}$$

For $k = 1$, the first truncated series is:

$$\mathfrak{B}_1(x,q) = \frac{e^x}{q} + \frac{\mathfrak{U}_1(x)}{q^{p+1}}. \tag{88}$$

Substituting into the first LRF and using Eq. (87) with $k = 1$, we need to compute the necessary derivatives. Since $\mathfrak{U}_0(x) = e^x$, we have:

$$\mathcal{D}_x\mathfrak{U}_0(x) = e^x, \tag{89}$$
$$\mathcal{D}_{xx}\mathfrak{U}_0(x) = e^x, \tag{90}$$
$$\mathcal{D}_{xxxx}\mathfrak{U}_0(x) = e^x. \tag{91}$$

Now, evaluating the limit condition:

$$\lim_{q\to\infty}\left(q^{p+1}\mathcal{LRES}_1(x,q)\right) = 0, \tag{92}$$

we obtain:

$$\mathfrak{U}_1(x) = e^x\frac{(r-4)}{q^{p+1}}. \tag{93}$$

For $k = 2$, the second truncated series is:

$$\mathfrak{B}_2(x,q) = \frac{e^x}{q} + \frac{e^x(r-4)}{q^{p+1}} + \frac{\mathfrak{U}_2(x)}{q^{2p+1}}. \tag{94}$$

We need to compute:

$$\mathcal{D}_x\mathfrak{U}_1(x) = e^x(r-4), \tag{95}$$
$$\mathcal{D}_{xx}\mathfrak{U}_1(x) = e^x(r-4), \tag{96}$$
$$\mathcal{D}_{xxxx}\mathfrak{U}_1(x) = e^x(r-4). \tag{97}$$

Solving $\lim_{q\to\infty}\left(q^{2p+1}\mathfrak{LRES}_2(x,q)\right) = 0$, we obtain:

$$\mathfrak{U}_2(x) = e^x\frac{(r-4)^2}{q^{2p+1}}. \tag{98}$$

For $k = 3$, the third truncated series is:

$$\mathfrak{B}_3(x,q) = \frac{e^x}{q} + \frac{e^x(r-4)}{q^{p+1}} + \frac{e^x(r-4)^2}{q^{2p+1}} + \frac{\mathfrak{U}_3(x)}{q^{3p+1}}. \tag{99}$$

We need to compute:

$$\mathcal{D}_x\mathfrak{U}_2(x) = e^x(r-4)^2, \tag{100}$$
$$\mathcal{D}_{xx}\mathfrak{U}_2(x) = e^x(r-4)^2, \tag{101}$$
$$\mathcal{D}_{xxxx}\mathfrak{U}_2(x) = e^x(r-4)^2. \tag{102}$$

Solving $\lim_{q\to\infty}\left(q^{3p+1}\mathfrak{LRES}_3(x,q)\right) = 0$, we obtain:

$$\mathfrak{U}_3(x) = e^x\frac{(r-4)^3}{q^{3p+1}}. \tag{103}$$

For $k = 4$, the fourth truncated series is:

$$\mathfrak{B}_4(x,q) = \frac{e^x}{q} + \frac{e^x(r-4)}{q^{p+1}} + \frac{e^x(r-4)^2}{q^{2p+1}} + \frac{e^x(r-4)^3}{q^{3p+1}} + \frac{\mathfrak{U}_4(x)}{q^{4p+1}}. \tag{104}$$

We need to compute:

$$\mathcal{D}_x\mathfrak{U}_3(x) = e^x(r-4)^3, \tag{105}$$
$$\mathcal{D}_{xx}\mathfrak{U}_3(x) = e^x(r-4)^3, \tag{106}$$
$$\mathcal{D}_{xxxx}\mathfrak{U}_3(x) = e^x(r-4)^3. \tag{107}$$

Solving $\lim_{q\to\infty}\left(q^{4p+1}\mathfrak{LRES}_4(x,q)\right) = 0$, we obtain:

$$\mathfrak{U}_4(x) = e^x\frac{(r-4)^4}{q^{4p+1}}. \tag{108}$$

For $k = 5$, the fifth truncated series is:

$$\mathfrak{B}_5(x,q) = \frac{e^x}{q} + \frac{e^x(r-4)}{q^{p+1}} + \frac{e^x(r-4)^2}{q^{2p+1}} + \frac{e^x(r-4)^3}{q^{3p+1}} + \frac{e^x(r-4)^4}{q^{4p+1}} + \frac{\mathfrak{U}_5(x)}{q^{5p+1}}. \tag{109}$$

We need to compute:

$$\mathcal{D}_x\mathfrak{U}_4(x) = e^x(r-4)^4, \tag{110}$$
$$\mathcal{D}_{xx}\mathfrak{U}_4(x) = e^x(r-4)^4, \tag{111}$$
$$\mathcal{D}_{xxxx}\mathfrak{U}_4(x) = e^x(r-4)^4. \tag{112}$$

Solving $\lim_{q\to\infty}\left(q^{5p+1}\mathfrak{LRES}_5(x,q)\right)=0$, we obtain:

$$\mathfrak{U}_5(x)=e^x\frac{(r-4)^5}{q^{5p+1}}. \tag{113}$$

In this way, the expansion-form solution of Eq. (80) in Laplace space is provided as

$$\begin{aligned}\mathfrak{B}(x,q)=&\frac{e^x}{q}+e^x\frac{(r-4)}{q^{p+1}}+e^x\frac{(r-4)^2}{q^{2p+1}}+e^x\frac{(r-4)^3}{q^{3p+1}}\\&+e^x\frac{(r-4)^4}{q^{4p+1}}+e^x\frac{(r-4)^5}{q^{5p+1}}+\cdots.\end{aligned} \tag{114}$$

By using the inverse L-T, we get an expansion solution in the original space:

$$\begin{aligned}F(x,t)=&e^x+e^x\frac{t^p}{\Gamma(p+1)}(r-4)+e^x\frac{t^{2p}}{\Gamma(2p+1)}(r-4)^2\\&+e^x\frac{t^{3p}}{\Gamma(3p+1)}(r-4)^3+e^x\frac{t^{4p}}{\Gamma(4p+1)}(r-4)^4\\&+e^x\frac{t^{5p}}{\Gamma(5p+1)}(r-4)^5+\cdots.\end{aligned} \tag{115}$$

The exact solution of Eq. (80) becomes as follows:

$$F(x,t)=e^x\mathbb{E}_p\left(t(r-4)\right), \tag{116}$$

where $\mathbb{E}_p(z)=\sum_{n=0}^{\infty}\frac{z^n}{\Gamma(np+1)}$ is the Mittag-Leffler function.

Remark 4.4. For the special case when $p=1$, the Mittag-Leffler function reduces to the exponential function, and the solution becomes $F(x,t)=e^xe^{t(r-4)}=e^{x+t(r-4)}$, which is the exact solution of the classical (integer-order) Swift-Hohenberg equation.

Problem 5. Consider the following non-linear, time FFPE:

$$\mathcal{D}_t^pF(x,t)+\mathcal{D}_x\left(\frac{4}{x}F^2(x,t)-\frac{x}{3}F(x,t)\right)-\mathcal{D}_{xx}F^2(x,t)=0, \tag{117}$$

where $t\geq 0$, $0\leq x\leq 1$, and $0<p\leq 1$, with the initial condition:

$$F(x,0)=x^2. \tag{118}$$

Applying the L-T to Eq. (117) and using the procedure explained in Section 3, we have

$$\begin{aligned}\mathfrak{B}(x,q)=&\frac{1}{q}x^2-\mathcal{D}_x\left(\frac{4}{x}\frac{1}{q^p}\mathfrak{L}_p\left[\mathfrak{L}_p^{-1}[\mathfrak{B}(x,q)]\right]^2-\frac{x}{3}\frac{1}{q^p}\mathfrak{B}(x,q)\right)\\&+\mathcal{D}_{xx}\left(\frac{1}{q^p}\mathfrak{L}_p\left[\mathfrak{L}_p^{-1}[\mathfrak{B}(x,q)]\right]^2\right),\end{aligned} \tag{119}$$

where $\mathfrak{L}_p[F(x,t)]=\mathfrak{B}(x,q)$ and $F(x,t)=\mathfrak{L}_p^{-1}[\mathfrak{B}(x,q)]$.

By using Lemma 2.3(c), we get

$$\mathfrak{U}_0(x)=\lim_{q\to\infty}\left(q\mathfrak{B}(x,q)\right)=F(x,0)=x^2. \tag{120}$$

The LRF is defined as

$$\begin{aligned}\mathfrak{LRES}(x,q) = \mathfrak{B}(x,q) - \frac{1}{q}x^2 \\ + \mathcal{D}_x\left(\frac{4}{x}\frac{1}{q^p}\mathfrak{L}_p\left[\mathfrak{L}_p^{-1}[\mathfrak{B}(x,q)]\right]^2 - \frac{x}{3}\frac{1}{q^p}\mathfrak{B}(x,q)\right) \\ - \mathcal{D}_{xx}\left(\frac{1}{q^p}\mathfrak{L}_p\left[\mathfrak{L}_p^{-1}[\mathfrak{B}(x,q)]\right]^2\right).\end{aligned} \tag{121}$$

The kth-truncated LRF takes the following form:

$$\begin{aligned}\mathfrak{LRES}_k(x,q) = \mathfrak{B}_k(x,q) - \frac{1}{q}x^2 \\ + \mathcal{D}_x\left(\frac{4}{x}\frac{1}{q^p}\mathfrak{L}_p\left[\mathfrak{L}_p^{-1}[\mathfrak{B}_k(x,q)]\right]^2 - \frac{x}{3}\frac{1}{q^p}\mathfrak{B}_k(x,q)\right) \\ - \mathcal{D}_{xx}\left(\frac{1}{q^p}\mathfrak{L}_p\left[\mathfrak{L}_p^{-1}[\mathfrak{B}_k(x,q)]\right]^2\right).\end{aligned} \tag{122}$$

Now, we construct the kth-truncated series solution in Laplace space. Note that for this problem, the series takes a slightly different form due to the initial condition x^2:

$$\mathfrak{B}_k(x,q) = \frac{x^2}{q} + \sum_{i=1}^{k}\frac{\mathfrak{U}_i(x)}{q^{ip+1}}. \tag{123}$$

To determine the coefficients $\mathfrak{U}_i(x)$, we solve the following equation:

$$\lim_{q\to\infty}\left(q^{kp+1}\mathfrak{LRES}_k(x,q)\right) = 0. \tag{124}$$

For $k = 1$, the first truncated series is:

$$\mathfrak{B}_1(x,q) = \frac{x^2}{q} + \frac{\mathfrak{U}_1(x)}{q^{p+1}}. \tag{125}$$

We need to compute the nonlinear terms. First, note that:

$$\mathfrak{L}_p^{-1}[\mathfrak{B}_1(x,q)] = x^2 + \mathfrak{U}_1(x)\frac{t^p}{\Gamma(p+1)} + \cdots \tag{126}$$

However, for the limit condition as $q \to \infty$, we only need the leading order terms. After substituting into the LRF and using Eq. (124) with $k = 1$, we obtain:

$$\mathfrak{U}_1(x) = x^2\frac{1}{q^{p+1}}. \tag{127}$$

For $k = 2$, the second truncated series is:

$$\mathfrak{B}_2(x,q) = \frac{x^2}{q} + \frac{x^2}{q^{p+1}} + \frac{\mathfrak{U}_2(x)}{q^{2p+1}}. \tag{128}$$

Solving $\lim_{q\to\infty}\left(q^{2p+1}\mathfrak{LRES}_2(x,q)\right) = 0$, we obtain:

$$\mathfrak{U}_2(x) = x^2\frac{1}{q^{2p+1}}. \tag{129}$$

For $k = 3$, the third truncated series is:

$$\mathfrak{B}_3(x,q) = \frac{x^2}{q} + \frac{x^2}{q^{p+1}} + \frac{x^2}{q^{2p+1}} + \frac{\mathfrak{U}_3(x)}{q^{3p+1}}. \tag{130}$$

Solving $\lim_{q\to\infty}\left(q^{3p+1}\mathfrak{LRES}_3(x,q)\right) = 0$, we obtain:

$$\mathfrak{U}_3(x) = x^2\frac{1}{q^{3p+1}}. \tag{131}$$

For $k = 4$, the fourth truncated series is:

$$\mathfrak{B}_4(x,q) = \frac{x^2}{q} + \frac{x^2}{q^{p+1}} + \frac{x^2}{q^{2p+1}} + \frac{x^2}{q^{3p+1}} + \frac{\mathfrak{U}_4(x)}{q^{4p+1}}. \tag{132}$$

Solving $\lim_{q\to\infty}\left(q^{4p+1}\mathfrak{LRES}_4(x,q)\right) = 0$, we obtain:

$$\mathfrak{U}_4(x) = x^2\frac{1}{q^{4p+1}}. \tag{133}$$

For $k = 5$, the fifth truncated series is:

$$\mathfrak{B}_5(x,q) = \frac{x^2}{q} + \frac{x^2}{q^{p+1}} + \frac{x^2}{q^{2p+1}} + \frac{x^2}{q^{3p+1}} + \frac{x^2}{q^{4p+1}} + \frac{\mathfrak{U}_5(x)}{q^{5p+1}}. \tag{134}$$

Solving $\lim_{q\to\infty}\left(q^{5p+1}\mathfrak{LRES}_5(x,q)\right) = 0$, we obtain:

$$\mathfrak{U}_5(x) = x^2\frac{1}{q^{5p+1}}. \tag{135}$$

In this way, the expansion-form solution of Eq. (117) in Laplace space is provided as

$$\mathfrak{B}(x,q) = \frac{x^2}{q} + \frac{x^2}{q^{p+1}} + \frac{x^2}{q^{2p+1}} + \frac{x^2}{q^{3p+1}} + \frac{x^2}{q^{4p+1}} + \frac{x^2}{q^{5p+1}} + \cdots. \tag{136}$$

By using the inverse L-T, we get an expansion solution in the original space:

$$\begin{aligned} F(x,t) = x^2 + x^2\frac{t^p}{\Gamma(p+1)} + x^2\frac{t^{2p}}{\Gamma(2p+1)} + x^2\frac{t^{3p}}{\Gamma(3p+1)} \\ + x^2\frac{t^{4p}}{\Gamma(4p+1)} + x^2\frac{t^{5p}}{\Gamma(5p+1)} + \cdots. \end{aligned} \tag{137}$$

The exact solution of Eq. (117) becomes as follows:

$$F(x,t) = x^2\mathbb{E}_p(t), \tag{138}$$

where $\mathbb{E}_p(t) = \sum_{n=0}^{\infty}\frac{t^{np}}{\Gamma(np+1)}$ is the Mittag-Leffler function.

Remark 4.5. For the special case when $p = 1$, the Mittag-Leffler function reduces to the exponential function, and the solution becomes $F(x,t) = x^2e^t$, which is the exact solution of the classical (integer-order) Fokker-Planck equation.

5 Numerical Simulation and Discussion

In this section, we present both graphical and numerical analyses of the App-S for the five nonlinear problems introduced in Section 4. To assess the accuracy and effectiveness of the proposed approximation technique, several error measures are employed. Since the LRPSM provides an approximate analytical solution in the form of an infinite fractional power series, it is essential to quantify the associated approximation errors. For this purpose, the Abs-E, Rel-E, and Res-E are computed to demonstrate the precision and reliability of the LRPSM.

Furthermore, we examine the graphical and numerical results of both the App-S and the corresponding exact solutions for Problems 1–5. Figures 1–5 display two-dimensional plots of the fifth-step App-S together with the exact solutions obtained via LRPSM for fractional orders $p = 0.6, 0.7, 0.8, 0.9$, and 1.0.

The graphical results clearly indicate that as $p \to 1.0$, the App-S approach the corresponding exact solution. The excellent agreement observed at $p = 1$ verifies the validity and robustness of the proposed method. For Problems 1–5, Figures 6–10 provide two-dimensional comparisons between the App-S and exact solutions through Abs-E analysis. The comparison confirms that the fifth-step App-S closely matches the exact solutions, and the Abs-E plots further demonstrate the high computational accuracy of the LRPSM.

Tables 1–5 present the Abs-E and Rel-E evaluated at selected points between the exact solutions and the fifth-step App-S obtained via LRPSM for Problems 1–5 at $p = 1.0$. The results indicate a strong agreement between the App-S and exact solutions, thereby validating the accuracy and effectiveness of the proposed method.

Tables 6–10 provide the Res-E associated with the fifth-step App-S over the interval $t \in [0, 0.5]$ for Problems 1–5 and fractional orders $p = 0.6, 0.7, 0.8, 0.9$, and 1.0. It is observed that the residual errors remain remarkably small across all cases, further confirming the precision, stability, and robustness of the proposed technique.

Overall, both the graphical and tabulated results demonstrate that the LRPSM is an efficient and reliable approach for solving nonlinear fractional-order differential equations. The method achieves high accuracy while requiring relatively fewer computational steps and iterations.

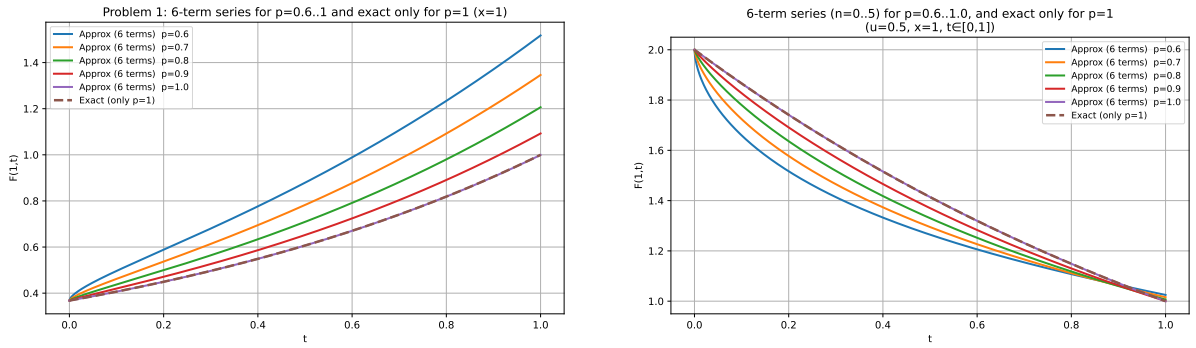

(a) Problem 1 at $x = 1.0$ **(b)** Problem 2 at $x = 1.0$, $u = 0.5$

Figure 1: Two-dimensional comparison between the App-S and the exact solutions for different fractional orders p over the interval $t \in [0, 1]$. Left: Problem 1 at $x = 1.0$. Right: Problem 2 at $x = 1.0$ and $u = 0.5$. The plots illustrate the influence of the fractional parameter p on the solution behavior.

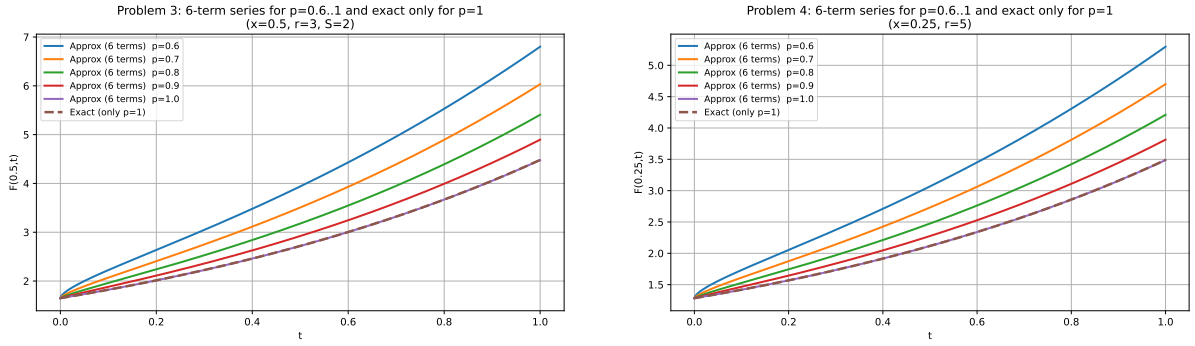

(a) Problem 3 at $x = 0.5$, $r = 3.0$, $S = 2.0$ **(b)** Problem 4 at $x = 0.25$, $r = 5.0$

Figure 2: Two-dimensional comparison of the App-S and the exact solutions for different fractional orders $p \in [0.6, 1.0]$. Left: Problem 3 with $x = 0.5$, $r = 3.0$, and $S = 2.0$. Right: Problem 4 with $x = 0.25$ and $r = 5.0$. The figures demonstrate the effect of the fractional parameter p on the solution dynamics.

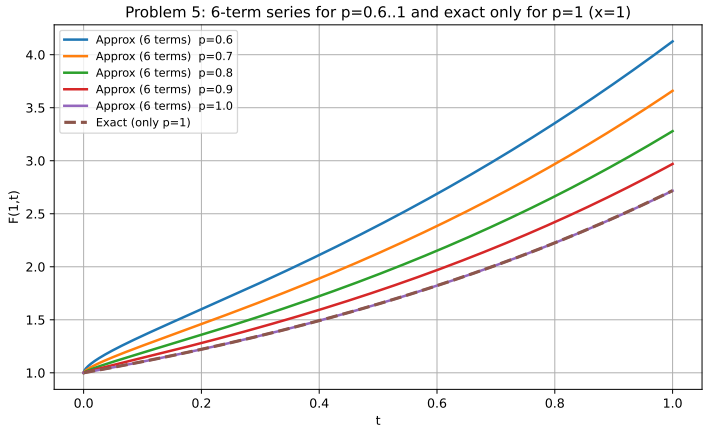

Figure 3: Two-dimensional plots comparing the App-S and the exact solution for Problem 5 at $x = 1.0$ over $t \in [0, 1]$. The figure illustrates the effect of the fractional order p on the solution behavior and confirms the high accuracy of the proposed approximation method.

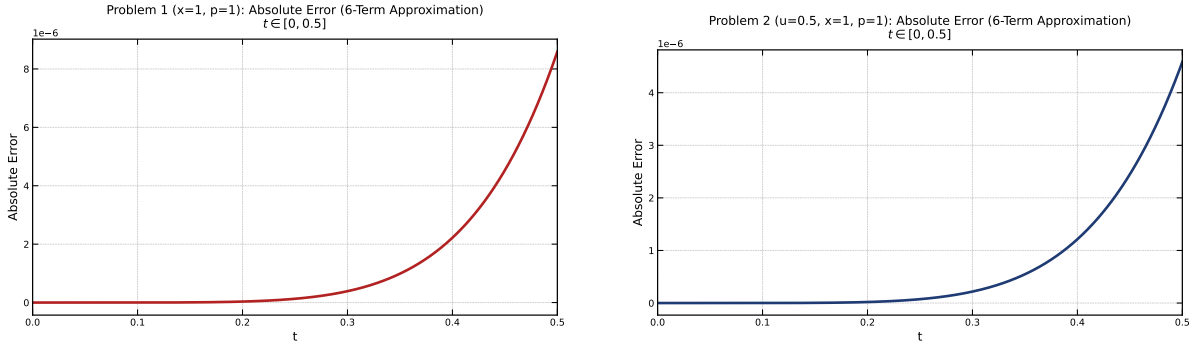

(a) Problem 1 at $p = 1.0$, $x = 1.0$ **(b)** Problem 2 at $p = 1.0$, $x = 1.0$, $u = 0.5$

Figure 4: Two-dimensional Abs-E plots comparing the fifth-step App-S and the exact solution for $p = 1.0$ over $t \in [0, 0.5]$. Left: Problem 1 at $x = 1.0$. Right: Problem 2 at $x = 1.0$ and $u = 0.5$. The plots demonstrate the high precision of the truncated approximation in the short-time interval.

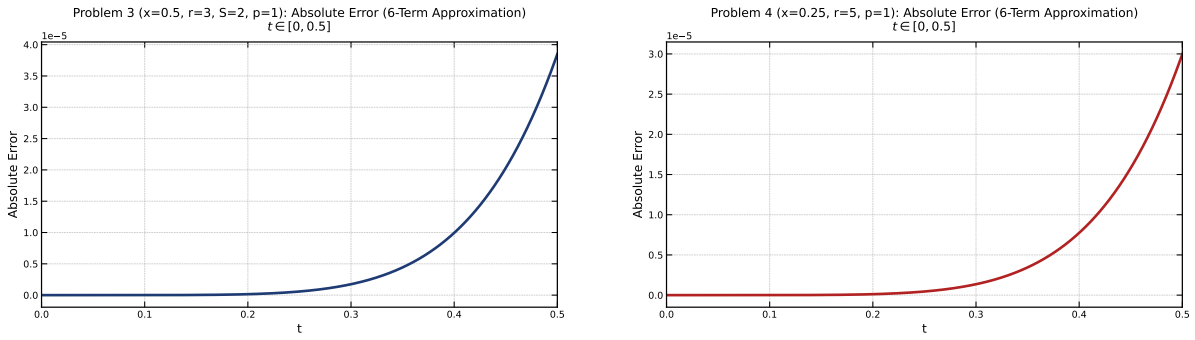

(a) Problem 3 at $p = 1.0$, $x = 0.5$, $r = 3.0$, $S = 2.0$ **(b)** Problem 4 at $p = 1.0$, $x = 0.25$, $r = 5.0$

Figure 5: Two-dimensional Abs-E between the App-S and the exact solution for $p = 1.0$ over the interval $t \in [0, 0.5]$. Left: Problem 3 with $x = 0.5$, $r = 3.0$, and $S = 2.0$. Right: Problem 4 with $x = 0.25$ and $r = 5.0$. The plots demonstrate the high accuracy of the truncated approximation in the short-time region.

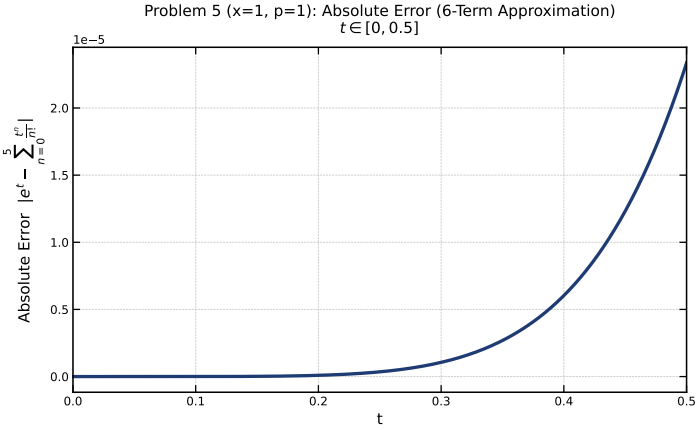

Figure 6: Two-dimensional Abs-E between the App-S and the exact solution for Problem 5 with $p = 1.0$ and $x = 0.5$ over the interval $t \in [0, 0.5]$. The graph confirms the high accuracy of the truncated approximation in the short-time region.

Table 1: Absolute and Relative Errors for Problem 1 at $x = 1.0$

t	$F(1,t)$	$F_5(1,t)$	Rel-E	Abs-E
0.1	0.4065696598	0.4065696592	1.27×10^{-9}	5.18×10^{-10}
0.2	0.4493289642	0.4493289305	7.49×10^{-8}	3.37×10^{-8}
0.3	0.4965853039	0.4965849147	7.83×10^{-7}	3.89×10^{-7}
0.4	0.5488116361	0.5488094174	4.04×10^{-6}	2.22×10^{-6}
0.5	0.6065306598	0.6065220682	1.42×10^{-5}	8.59×10^{-6}
0.6	0.6703200461	0.6702940000	3.89×10^{-5}	2.60×10^{-5}
0.7	0.7408182207	0.7407515275	9.00×10^{-5}	6.67×10^{-5}
0.8	0.8187307531	0.8185798262	1.84×10^{-4}	1.51×10^{-4}
0.9	0.9048374181	0.9045266110	3.43×10^{-4}	3.11×10^{-4}
1.0	1.0000000000	0.9994058154	5.94×10^{-4}	5.94×10^{-4}

Table 2: Absolute and Relative Errors for Problem 2 at $x = 1.0$, $u = 0.5$

t	$F(1,t)$	$F_5(1,t)$	Rel-E	Abs-E
0.1	1.866065983	1.866065983	1.63×10^{-10}	3.05×10^{-10}
0.2	1.741101107	1.741101127	1.11×10^{-8}	1.93×10^{-8}
0.3	1.624504575	1.624504793	1.34×10^{-7}	2.18×10^{-7}
0.4	1.515715353	1.515716567	8.00×10^{-7}	1.21×10^{-6}
0.5	1.414208977	1.414213562	3.24×10^{-6}	4.59×10^{-6}
0.6	1.319494349	1.319507911	1.03×10^{-5}	1.36×10^{-5}
0.7	1.188443101	1.231144413	3.47×10^{-2}	4.27×10^{-2}
0.8	1.148623576	1.148698355	6.51×10^{-5}	7.48×10^{-5}
0.9	1.071623268	1.071773463	1.40×10^{-4}	1.50×10^{-4}
1.0	0.999719982	1.000000000	2.80×10^{-4}	2.80×10^{-4}

Table 3: Abs-E and Rel-E at varying values of (x,t) with $r = 3.0$ and $S = 2.0$ for Problem 3

(x,t)	$F_5(x,t)$	$F(x,t)$	Rel-E	Abs-E
(0.03,0.03)	1.06183654654432	1.06183654654535	$9.865985960312 \times 10^{-13}$	$1.0476064460362 \times 10^{-12}$
(0.13,0.13)	1.29693007888701	1.29693008666577	$5.9977915677191 \times 10^{-9}$	$7.7787163377252 \times 10^{-9}$
(0.23,0.23)	1.58407371746601	1.58407398499448	$1.6888630985918 \times 10^{-7}$	$2.6752840986965 \times 10^{-7}$
(0.33,0.33)	1.93478971675811	1.93479233440203	$1.352932710503 \times 10^{-6}$	$2.6176438372431 \times 10^{-6}$
(0.43,0.43)	2.36314632122551	2.36316069370579	$6.081888669505 \times 10^{-6}$	$1.43724802472712 \times 10^{-5}$
(0.53,0.53)	2.88631445113781	2.88637098926795	$1.9587963696605 \times 10^{-5}$	$5.65381301527101 \times 10^{-5}$
(0.63,0.63)	3.52524252279690	3.52542148736538	$5.0764020450205 \times 10^{-5}$	$1.78964568480211 \times 10^{-4}$
(0.73,0.73)	4.30547337653070	4.30595952834520	$1.12902086352814 \times 10^{-4}$	$4.861518145009562 \times 10^{-4}$
(0.83,0.83)	5.25813191201622	5.25931084444689	$2.24161009976689 \times 10^{-4}$	$1.1789324306725742 \times 10^{-3}$
(0.93,0.93)	6.42111750626145	6.42373677142913	$4.07747898283598 \times 10^{-4}$	$2.6192651676772981 \times 10^{-3}$

Table 4: Abs-E and Rel-E at varying values of (x,t) with $r = 3.0$ for Problem 4

(x,t)	$F_5(x,t)$	$F(x,t)$	Rel-E	Abs-E
(0.05,0.05)	1.05127109637602	1.05127109637625	2.1875×10^{-13}	2.3026×10^{-13}
(0.15,0.15)	1.16183424272828	1.16183424500371	1.9579×10^{-9}	2.2754×10^{-9}
(0.25,0.25)	1.28402541668774	1.28402548777896	5.5375×10^{-8}	7.1091×10^{-8}
(0.35,0.35)	1.41906753061577	1.41906824523260	5.0359×10^{-7}	7.1462×10^{-7}
(0.45,0.45)	1.56831218549017	1.56831666142069	2.8536×10^{-6}	4.4759×10^{-6}
(0.55,0.55)	1.73324575681559	1.73326557360500	1.1432×10^{-5}	1.9817×10^{-5}
(0.65,0.65)	1.91550935671475	1.91557751702737	3.5568×10^{-5}	6.8160×10^{-5}
(0.75,0.75)	2.11691862097731	2.11711249324624	9.1553×10^{-5}	1.9387×10^{-4}
(0.85,0.85)	2.33948772933147	2.33996123388635	2.0240×10^{-4}	4.7350×10^{-4}
(0.95,0.95)	6.6661756508830	6.6858944422792	2.9493×10^{-3}	$1.9718791396183377 \times 10^{-2}$

Table 5: Abs-E and Rel-E at varying values of t when $x = 1.0$ for Problem 5

t	$F(1,t)$	$F_5(1,t)$	Rel-E	Abs-E
0.1	0.27629272951891193	0.27629272916666664	$1.274898869421280 \times 10^{-9}$	$3.522452884929805 \times 10^{-10}$
0.2	0.30535068954004246	0.30535066666666666	$7.490854479152386 \times 10^{-8}$	$2.287337580453297 \times 10^{-8}$
0.3	0.33746470189400080	0.33746443750000000	$7.834715729382329 \times 10^{-7}$	$2.643940008040246 \times 10^{-7}$
0.4	0.37295617441031760	0.37295466666666666	$4.042683174006208 \times 10^{-6}$	$1.507743650930315 \times 10^{-6}$
0.5	0.41218031767503205	0.41217447916666666	$1.4164937322380167 \times 10^{-5}$	$5.838508365385575 \times 10^{-6}$
0.6	0.45552970009762720	0.45551200000000003	$3.8856078151216220 \times 10^{-5}$	$1.770009762719349 \times 10^{-5}$
0.7	0.50343817686761920	0.50339285416666660	$9.002634888475257 \times 10^{-5}$	$4.532270095258806 \times 10^{-5}$
0.8	0.55638523212311700	0.55628266666666670	$1.8434252120403096 \times 10^{-4}$	$1.0256545645026538 \times 10^{-4}$
0.9	0.61490077778923750	0.61468956250000000	$3.4349491310922605 \times 10^{-4}$	$2.1121528923750965 \times 10^{-4}$
1.0	0.67916666672122200	0.67916666666666670	$3.9349491310922605 \times 10^{-4}$	$2.9166666666666700 \times 10^{-4}$

6 Conclusion

In this study, we developed an efficient hybrid analytical technique known as the LRPSM for solving nonlinear time-fractional partial differential equations involving the Caputo derivative. The proposed approach combines the advantages of the L-T and the Residual Power Series Method to construct approximate and exact solutions in a systematic and computationally efficient manner.

The method was successfully applied to five nonlinear fractional models, including gas dynamics equations, Swift–Hohenberg equations, and a fractional Fokker–Planck equation. The obtained solutions were expressed in terms of fractional power series and corresponding closed-form representations involving the Mittag–Leffler function.

To validate the effectiveness and reliability of the proposed technique, absolute errors, relative errors, and residual errors were computed and analyzed both numerically and graphically. The results demonstrate strong agreement between the approximate solutions and the corresponding exact solutions. Furthermore, as the fractional order $p \to 1$, the approximate solutions converge to the classical integer-order solutions, confirming the consistency of the method.

The residual error analysis shows that LRPSM produces highly accurate results with fewer computational steps compared to traditional analytical methods such as the Adomian Decomposition Method, Variational Iteration Method, and Homotopy Perturbation Method.

Overall, LRPSM provides a simple, reliable, and efficient framework for solving nonlinear fractional differential equations and can be extended to more complex fractional systems arising in physics, biology, engineering, and applied sciences.

Declarations

Funding

This research received no external funding.

Competing Interests

Not applicable.

Ethical Approval

Not applicable.

Authors's Contributions

Not applicable.

Availability Data and Materials

The data contained in the article.

Acknowledgements

The authors would like to thank the editors and reviewers for their time, effort, and valuable commentswhich led to improvements in our manuscript.

Abbreviations

The following abbreviations are used in this manuscript:

FDEs	fractional differential equations
PDEs	partial Differential Equations
Abs-E	absolute error
Rel-E	relative error
Res-E	residual error
App-S	approximate solutions
RPSM	residual power series method
L-T	Laplace transform
FGDE	fractional gas dynamics equation
FFPE	fractional Fokker-Planck equation
SHE	Swift-Hohenberg equation
CFD	Caputo fractional derivative

References

[1] S. A. Almutlak, R. Shah, W. Weera, S. A. El-Tantawy, and L. S. El-Sherif, *Fractional view analysis of Swift–Hohenberg equations by an analytical method and some physical applications*, Fractal Fract. **6** (2022), 524.

[2] A. H. Bhrawy and A. S. Alofi, *The operational matrix of fractional integration for shifted Chebyshev polynomials*, Appl. Math. Lett. **26** (2013), 25–31.

[3] S. Das and R. Kumar, *Approximate analytical solutions of fractional gas dynamic equations*, Appl. Math. Comput. **217** (2011), 9905–9915.

[4] S. Hasan, A. El-Ajou, S. Hadid, M. Al-Smadi, and S. Momani, *Atangana–Baleanu fractional framework of reproducing kernel technique in solving fractional population dynamics system*, Chaos Solitons Fractals **133** (2020), 109624.

[5] H. K. Jassim and M. G. Mohammed, *Natural homotopy perturbation method for solving nonlinear fractional gas dynamics equations*, Int. J. Nonlinear Anal. Appl. **12** (2021), 812–820.

[6] M. I. Liaqat, A. Akgül, and H. Abu-Zinadah, *Analytical investigation of some time-fractional Black–Scholes models by the Aboodh residual power series method*, Mathematics **11** (2023), 276.

[7] M. I. Liaqat, S. Etemad, S. Rezapour, and C. Park, *A novel analytical Aboodh residual power series method for solving linear and nonlinear time-fractional partial differential equations with variable coefficients*, AIMS Math. **7** (2022), 16917–16948.

[8] M. I. Liaqat, A. Khan, M. A. Alam, and M. K. Pandit, *A highly accurate technique to obtain exact solutions to time-fractional quantum mechanics problems with zero and nonzero trapping potential*, J. Math. (2022), Article ID not provided.

[9] A. M. Mahdy, *Numerical solutions for solving model time-fractional Fokker–Planck equation*, Numer. Methods Partial Differ. Equ. **37** (2021), 1120–1135.

[10] S. Maitama and W. Zhao, *New homotopy analysis transform method for solving multidimensional fractional diffusion equations*, Arab J. Basic Appl. Sci. **27** (2020), 27–44.

[11] K. Nonlaopon, A. M. Alsharif, A. M. Zidan, A. Khan, Y. S. Hamed, and R. Shah, *Numerical investigation of fractional-order Swift–Hohenberg equations via a novel transform*, Symmetry **13** (2021), 1263.

[12] S. C. Shiralashetti and A. B. Deshi, *An efficient Haar wavelet collocation method for the numerical solution of multi-term fractional differential equations*, Nonlinear Dyn. **83** (2016), 293–303.

[13] M. Tamsir and V. K. Srivastava, *Revisiting the approximate analytical solution of fractional-order gas dynamics equation*, Alexandria Eng. J. **55** (2016), 867–874.

[14] K. Vishal, S. Das, S. H. Ong, and P. Ghosh, *On the solutions of fractional Swift–Hohenberg equation with dispersion*, Appl. Math. Comput. **219** (2013), 5792–5801.

[15] J. L. Wei, G. C. Wu, B. Q. Liu, and Z. Zhao, *New semi-analytical solutions of the time-fractional Fokker–Planck equation by the neural network method*, Optik **259** (2022), 168896.